Estrogen promotes the brain metastatic colonization of triple negative breast cancer cells via an astrocyte-mediated paracrine mechanism

Carol A. Sartorius[1], Colton T. Hanna[1], Brunilde Gril[4], Hazel Cruz[1], Natalie J. Serkova[2], Kendra M. Huber[2], Peter Kabos[3], Troy B. Schedin[3], Virginia F. Borges[3], Patricia S. Steeg[4], and Diana M. Cittelly[1,*]

[1]Department of Pathology, University of Colorado Denver, Anschutz Medical Campus, Aurora, CO, 80045

[2]Department of Anesthesiology, University of Colorado Denver, Anschutz Medical Campus, Aurora, CO, 80045

[3]Department of Medicine, Division of Medical Oncology, University of Colorado Denver, Anschutz Medical Campus, Aurora, CO, 80045

[4]Women's Malignancies Branch, National Cancer Institute, Bethesda, MD, 20892, USA

Abstract

Brain metastases (BM) are a devastating consequence of breast cancer. BM occur more frequently in patients with estrogen receptor-negative (ER−) breast cancer subtypes; HER2 overexpressing (HER2+) tumors and triple-negative (TN) (ER−, progesterone receptor-negative (PR−) and normal HER2) tumors. Young age is an independent risk factor for development of BM, thus we speculated that higher circulating estrogens in young, pre-menopausal women could exert paracrine effects through the highly estrogen-responsive brain microenvironment. Using a TN experimental metastases model, we demonstrate that ovariectomy decreased the frequency of MRI detectable lesions by 56% as compared to estrogen supplementation, and that the combination of ovariectomy and letrozole further reduced the frequency of large lesions to 14.4% of the estrogen control. Human BM expressed 4.2-48.4% ER+ stromal area, particularly ER+ astrocytes. *In vitro*, E2-treated astrocytes increased proliferation, migration and invasion of 231BR-EGFP cells in an ER-dependent manner. E2 upregulated EGFR ligands *Egf, Ereg,* and *Tgfa* mRNA and protein levels in astrocytes, and activated EGFR in brain metastatic cells. Co-culture of 231BR-EGFP cells with E2-treated astrocytes led to upregulation of the metastatic mediator S100 Calcium-binding protein A4 (S100A4) (1.78-fold, P<0.05). Exogenous EGF increased S100A4 mRNA

*Correspondence: 12801 E 17th Ave. MS8104, University of Colorado Denver, Anschutz Medical Campus, Aurora, CO, 80045. 303-724-8343, Diana.Cittelly@ucdenver.edu.

levels in 231BR-EGFP cells (1.40±0.02 fold, P<0.01 compared to vehicle-control) and an EGFR/ HER2 inhibitor blocked this effect, suggesting that S100A4 is a downstream effector of EGFR activation. ShRNA-mediated S100A4 silencing in 231BR-EGFP cells decreased their migration and invasion in response to E2-CM, abolished their increased proliferation in co-cultures with E2-treated astrocytes, and decreased brain metastatic colonization. Thus, S100A4 is one effector of the paracrine action of E2 in brain metastatic cells. These studies provide a novel mechanism by which estrogens, acting through ER+ astrocytes in the brain microenvironment, can promote BM of TN breast cancers, and suggests existing endocrine agents may provide some clinical benefit towards reducing and managing BM.

Keywords

breast cancer; brain metastasis; estrogen; estrogen receptors; astrocytes; EGF

INTRODUCTION

Symptomatic brain metastases (BM) develop in 10 to 16% of patients with metastatic breast cancer and the prognosis of these patients is dismal with a survival varying from 4 to 18 months with multimodal therapies (1-3). The highest incidence of BM occurs in breast cancers overexpressing HER2 (HER2+), and triple negative (TN) breast cancers (negative for estrogen receptor (ER), progesterone receptor (PR), and normal HER2) (4-9). There are currently no effective targeted therapies for TN tumors, and large antibodies targeting HER2+ tumors have limited ability to cross the blood-brain barrier (BBB). Estrogens are the main mitogens driving the growth of ER+ breast cancers, and thus these tumors are treated with endocrine targeting agents such as tamoxifen (a selective estrogen modulator (SERM)), fulvestrant (ICI) (a selective estrogen degrader (SERD)), and aromatase inhibitors (AIs) such as letrozole which block the enzyme that produces estrogens. Since the vast majority of breast cancers that colonize the brain are from ER− subtypes, it has been assumed that estrogens do not play a role in their clinical course. However, TN and HER2+ breast cancers are more prevalent in pre-menopausal women, and young age (<40) is an independent risk factor for developing central nervous system (CNS) metastasis (6, 9-15). This suggests that a brain microenvironment fueled by estrogen might play a role in the development of ER− BM.

The brain microenvironment is highly estrogen-responsive as astrocytes, neurons, endothelial cells and microglia express classical ERs (ERα and ERβ) as well as non-classical G-protein coupled receptor 30 (GPR30) (16-19). Estrogens play lifelong roles in the formation, maintenance, and remodeling of neuronal circuits in the brain (17, 20-22). As estrogens are small lipophilic molecules, they readily diffuse through the multiple cell membranes that comprise the BBB to penetrate the CNS. In pre-menopausal women the brain is exposed to peak estrogen levels during the follicular phase; in the absence of ovarian estrogens, the brain is not completely estrogen-depleted due to local synthesis by aromatase-expressing astrocytes (23-25). We hypothesized that estrogen acting through the brain microenvironment would influence the ability of ER− breast cancer cells to colonize the brain, and investigated the preventive effect of ovarian and peripheral estrogen depletion

using an experimental model of TN breast cancer BM. We demonstrate that 17-β-estradiol (E2) stimulates the release of astrocyte-derived paracrine factors that promote the proliferation, migration, and invasion of TN brain metastatic cells. We provide a novel mechanism by which estrogens indirectly affect the brain metastatic colonization of TN breast cancer cells. These findings could have significant translational effects as aromatase inhibitors used to treat ER+ breast tumors can cross the blood brain barrier.

RESULTS

Estrogen depletion decreases brain metastatic colonization of the ER− brain tropic cell line 231BR-EGFP

To determine whether estrogens affect the ability of ER− cells to colonize the brain, we utilized the well characterized brain-tropic subline of human TN MDA-MB-231 breast cancer cells, termed 231-BR-EGFP (26, 27). These cells form high frequencies of BM when introduced into the circulation of immune compromised mice. For our experiments, ovariectomized (OVX) female nu/nu mice were implanted with slow release pellets containing 1mg E2 (E2) or placebo. OVX mice supplemented with placebo pellets were additionally injected with vehicle-control (OVX) or 10 μg of letrozole daily (OVX +Letrozole). Two days post endocrine initiation, 231-BR-EGFP cells were introduced via intracardiac (ic) injection. Macroscopic BM were quantified using T2-weighted and gadolinium enhanced T1-weighted magnetic resonance imaging (MRI) at 25 to 28 days post injection and sacrificed thereafter. While 62.5% (10/16) of E2-treated mice developed MRI detectable metastases (>0.2mm), only 35.2% (6/17) of OVX mice and 9% (1/11) of OVX +letrozole treated mice developed large BM, a reduction to 56% and 14.4% as compared to E2-treated mice, respectively (P=0.0186, χ^2 test) (Figure 1a). . The mean number of MRI detectable metastases showed similar trends, 1.37 in estrogen treated controls as compared to 0.4 (P=0.043) in OVX and 0.18 (P=0.0089) in OVX + Letrozole (Figure 1a). Median diameter of MRI-detectable metastases was 0.54 mm (range 0.2-2.97 mm) in E2-treated mice, 0.3 mm (range 0.2-1.64 mm) in OVX, and <0.2 mm in OVX+Letrozole mice (Figure 1b). Occult micrometastases were quantified in step sections through one brain hemisphere based on a cutoff of 300 μm along the longest axis (26). Ovarian estrogen depletion alone (OVX) resulted in a median of 17.5 micrometastases per section, and OVX+Letrozole mice showed a median of 21 micrometastases per section, a reduction of 64% and 56% compared to E2-treated mice (48.5 median number of micrometastases per section, P=0.0001 and P=0.0098 respectively, Figure 1c). These data demonstrate that ovarian estrogen and, to a lesser extent, peripheral estrogen, play a role in brain metastatic colonization of otherwise estrogen unresponsive TN breast cancer cells.

Astrocytes proximal to breast cancer BM are ER+ in patients and xenograft models

BM are surrounded and infiltrated by activated astrocytes (expressing Glial Fibrillary Acidic Protein, GFAP), part of the neuro-inflammatory response to metastases in the brain microenvironment (26). We assessed expression of estrogen receptors ERα and ERβ in the tumor microenvironments of sections of clinical resected breast cancer metastases and in experimental 231BR-EGFP BM. Clinically stained sections of BM (n=12) contained ERα+ stroma, with a 75% percentile of 19.89% (mean 15.85±12.25%) positive stromal area,

plotted according to different subtypes (Figure 2a, Supplementary Figure 1). Double-immunofluorescence staining showed that this ER+ tumor associated stroma includes GFAP + astrocytes, expressing both ERα and ERβ (Figure 2b). Nuclear and membrane localized expression of ERα and ERβ was observed also in activated astrocytes (GFAP+) surrounding metastatic lesions the 231BR-EGFP model (Figure 2c). These data support the hypothesis that the astrocytic brain microenvironment can mediate estrogen signals in the context of breast cancer BM.

E2-treated astrocytes increase proliferation, migration and invasion of brain metastatic cells in an ER-dependent manner

We hypothesized that estrogens could signal through astrocytes in the neuroinflammatory response to increase breast cancer cell brain colonization. To test this, we used primary mouse astrocytes isolated from neonatal mice which contain >95% GFAP+ cells, and human astrocytes differentiated from the human neural stem cell line K048 (28). Both murine and human astrocytes stained positive for nuclear and membrane localized ERα and ERβ (Figure 2d, Supplementary Figure 2a). Neither human nor mouse-derived astrocytes contained detectable levels of non-classical estrogen receptor membrane associated GPR30. The 231BR-EGFP cells lack ERα (Figure 2d), have low levels of ERβ and are unresponsive to E2, as measured by proliferation, migration, and invasion (Figure 3a, b, & c).

To determine if E2 could exert paracrine actions though astrocytes and influence breast cancer cells, we used a co-culture system. Co-culture with astrocytes led to increased proliferation of 231BR-EGFP cells in E2 as compared to vehicle-treated samples ($20.12\pm1.8\%$ GFP+ cells in E2 vs $14.8\pm2.5\%$ GFP+ in vehicle cells after 6 days, $P<0.0001$) (Figure 3a). The selective ER antagonist 4-hydroxy-tamoxifen (4OH-TAM) and pure-anti ERα and ERβ ICI were used for *in vitro* experiments, as letrozole was ineffective in serum-free culture medium. Both agents blocked the increase in E2-mediated proliferation (10.1 ± 2.4 and $14.9\pm2.4\%$ GFP+ cells after 6 days, respectively, $P<0.0001$) (Figure 3a). No difference in ER expression of astrocytes was noted under these conditions (data not shown). These data suggest that the paracrine effects of E2 on 231BR-EGFP cell proliferation are dependent on astrocytic ERs.

Since the establishment of metastases depends to a great extent on the ability of cells to migrate and invade through the extracellular matrix, we determined whether E2 paracrine factors released from astrocytes could alter the migratory and invasive ability of 231BR-EGFP cells. Concentrated conditioned media (CM) from E2-treated astrocytes (CM-E2) increased migration of 231BR-EGFP cells in a scratch wound assay (29.1 ± 58.1 μm wound at 24 h), as compared to CM from vehicle-treated astrocytes (CM-OH) (196.9 ± 35.7 μm wound at 24 h, $P<0.0001$) (Figure 3b). CM from astrocytes treated with E2 in combination with 4-hydroxy-tamoxifen (CM E2+4-OH-TAM) and ICI (CM E2+ICI) abolished this effect (149.7 ± 30.41 μm and 133.6 ± 10.9 μm, $P<0.01$ and $P<0.05$ compared to CM-E2, respectively) suggesting that paracrine effects of E2 on 231BR-EGFP migration are dependent on astrocytic ERs (Figure 3b). A modified scratch wound assay was used to assess the ability of 231BR-EGFP cells to invade through a Matrigel-filled wound, and the relative wound density (RWD) over time was assessed using IncuCyte live imaging. CM-E2

significantly increased invasion of 231BR-EGFP cells (85.3±1.6% RWD at 24 h) as compared to CM-OH (72.6%1.6 RWD at 24 h) (P<0.0001), and CM-4OH-TAM and CM-ICI abolished this effect (73.8.7±3.8% and 73.3±3.2% at 24 h, P<0.001 compared to CM-E2) (Figure 3c). We confirmed these results by demonstrating 231BR-EGFP cells invade through Matrigel-coated Boyden chambers, with E2– but not vehicle-treated astrocyte CM as a chemoattractant (Supplementary Figure 3). Despite the expression of ERβ in 231BR-EGFP cells, the same treatments had no effect on proliferation, migration or invasion in the absence of astrocytes (data not shown). These results implicate that E2 can work through astrocytic ERs to increase 231BR-EGFP cell migration, invasion and proliferation.

E2 upregulates EGFR ligands in astrocytes leading to EGFR activation and increased migration and invasion of 231BR-EGFP cells

Transforming growth factor-alpha (TGFα) is abundant in astrocytes and its expression increases in response to E2 (29, 30). TGFα is an EGFR-ligand, and EGFR expression was increased in human brain metastasis (6,10). EGFR activation is also a well-known mechanism driving migration, invasion and proliferation of metastatic cells, so we sought to elucidate whether TGFα and other EGFR ligands are in part responsible for the paracrine effects of E2 in brain metastatic cells. Tgfα and Ereg mRNA levels were modestly upregulated following E2– treatment of mouse astrocytes (1.5±0.3 fold increase at 48 h, P<0.05) while Egf mRNA levels were robustly upregulated at 6 and 48 h after E2-stimulation (3.4±0.4 fold change at 6 h and 4.2±0.6 fold change at 48 h, P<0.05) (Figure 4a). Co-treatment with E2 plus 4OH-Tam or ICI abolished E2-mediated mRNA upregulation for all ligands (Figure 4b). Upregulation of EGF and TGFα was also observed in E2-treated human astrocytes (Supplementary Figure 2b). EGF and EREG protein levels were significantly increased in E2-treated astrocytes (6.2±2.4 and 2.3±0.4 fold increase, respectively, P<0.05), as compared to OH-treated astrocytes, and both 4-OH-TAM and ICI abolished this effect (Figure 4c). TGFα precursor measured by western blot, also showed a 3-fold increase in TGFα protein levels in E2-treated compared to vehicle-treated astrocytes, with only a moderate blockage by 4-OH-TAM and complete blockage with ICI (Figure 4c). Taken together these results suggest that E2-mediated upregulation of Egf, Tgfα and Ereg in astrocytes is dependent on ERs.

231BR-EGFP cells express high levels of EGFR and EGFR activation drives migration and invasion in this cell line (31). Thus, we asked whether CM from E2-stimulated astrocytes could activate EGFR in 231BR-EGFP cells, and whether EGFR activation is a downstream effector for astrocytic ligands that increase the aggressive behavior of 231BR-EGFP cells in response to CM-E2. Since the EGFR/HER inhibitor lapatinib has been shown to reduce EGFR activation and downstream signaling in 231BR-EGFP cells *in vitro* (31), we used lapatinib to block EGFR activation in response to CM-E2 and measure its role in migration and invasion. Treatment of 231BR-EGFP cells with CM-E2 but not CM-OH resulted in EGFR phosphorylation (Y1068) and lapatinib abolished this effect (Figure 4d). Treatment with media containing OH or E2 alone, did not lead to EGFR phosphorylation (data not shown), suggesting that the residual E2 present in the CM is not directly responsible for EGFR phosphorylation. Lapatinib inhibited the increase in migration and invasion of

231BR-EGFP cells in response to CM-E2, suggesting a role for EGFR activation in mediating paracrine effects of E2 (Figure 4d).

The metastasis mediator S100A4 is a downstream effector of astrocyte activated EGFR in 231BR-EGFP cells

We next measured global gene expression of 231BR-EGFP co-cultured for 24hr with astrocytes pre-treated with vehicle or 10 nM E2 for 24 h. E2 treatment in the absence of astrocytes did not alter gene expression profiles, confirming that E2 does not directly affect gene expression in 231BR-EGFP cells. We identified 254 genes that were differentially expressed (fold change >1.5 and p<0.05) in 231BR-EGFP cells in co-culture with E2-stimulated (E2^{Astro}/231BR) compared to OH-stimulated astrocytes (OH^{Astro}/231BR) (Figure 5a, Supplementary Table 1). The S100 Calcium-binding protein A4 (S100A4) was significantly upregulated (1.78 fold change, P<0.05) in E2^{Astro}/231BR cells as compared to OH^{Astro}/231BR. qRT-PCR confirmed the mRNA upregulation of S100A4 in E2^{Astro} 231BR-EGFP cells (6.6±1.7 vs. 1.8±1.4 fold increase in E2 vs OH treated-respectively, P<0.05), and treatment of astrocytes with E2+ICI abolished this effect (1.5±0.3 fold increase, P<0.05 vs E2^{Astro}-treated) (Figure 5b), suggesting that S100A4 upregulation depends on E2-ER signaling in astrocytes.

We next determined whether S100A4 mRNA upregulation in 231BR-EGFP cells was dependent on EGFR activation. 231BR-EGFP cells were pretreated with vehicle or lapatinib for 6 h, then treated with EGF or vehicle (OH) for an additional 48 h. EGF upregulated S100A4 mRNA levels in 231BR-EGFP cells (1.40±0.02 fold increase in EGF-treated vs 1.0±0.07 fold in DMSO-control, P<0.01) (Figure 5c), and lapatinib decreased this effect (1.13±0.05 fold change in EGF/LAP treated cells), suggesting that S100A4 is a downstream effector of EGFR activation in 231BR-EGFP cells.

As S100A4 is important in promoting proliferation, migration and metastasis (32, 33), we sought to elucidate the role of S100A4 in mediating the E2-stimulated increases in proliferation, migration and invasion of 231BR-EGFP cells. Three different shRNA lentiviral vectors (sh6308, sh6309, sh6310) were used to knockdown S100A4 expression in 231BR-EGFP cells. All shRNAs were able to abolish the upregulation of S100A4 in response to E2-treated astrocytes (Figure 6a, Supplementary Figure 4), compared to scramble-control shRNA (Sh-NC) cells. Furthermore, S100A4 inhibition blocked the increases in migration (Figure 6b), invasion (Figure 6c) and proliferation (Figure 6d) of 231BR-EGFP cells in response to E2-treated astrocytes S100A4 knockdown also significantly decreased the ability of 231BR-EGFP cells to proliferate in response to EGF (Figure 6e), further supporting S100A4 as an effector downstream of EGFR activation. ShS100A4-231BR (sh6309) cells showed a significant decrease in its ability to form metastases in E2-treated mice (median number of metastases 0), as compared to shNC cells (median number of metastases 48, P<0.0001) (Figure 6f). Taken together, these data suggest that S100A4 is a key mediator of the paracrine effects of estrogen in 231BR cells.

Discussion

Elucidating the participation of the brain microenvironment during the brain metastatic process is of crucial importance for the identification of therapeutic and preventive alternatives. Despite the well-known role of estrogen in normal brain functioning (22, 34), the effects of ovarian and local estrogens in the context of brain metastatic progression remain unknown. Our studies showing that estrogen supplementation to levels found in pre-menopausal women significantly increase brain metastatic colonization in the 231-BR-EGFP experimental model, are first to demonstrate a role for estrogen in brain metastatic colonization of TN breast cancer cells. We used both MRI-based quantification of large brain metastases and histological count of micrometastases to measure the contribution of ovarian and peripheral estrogen to brain metastatic colonization. Micromestases count did not show any added effect of letrozole to ovariectomy in preventing brain colonization. However, addition of letrozole was more effective than ovariectomy alone in decreasing the frequency and size of MRI-detectable metastases to 14.4% of E2-treated mice (compared to a reduction of 56% by ovariectomy alone). This suggests that in the absence of ovarian estrogen (i.e in post-menopausal women), locally produced estrogen plays a role in promoting the growth of brain metastatic cells.

E2 has been previously shown to accelerate the growth of ER− patient-derived xenograft tumors by influencing the mobilization and recruitment of a pro-angiogenic population of bone marrow–derived myeloid cells to the tumor microenvironment and increasing angiogenesis (35, 36). However, brain metastatic colonization of breast cancer does not necessarily rely on neo-angiogenesis (37, 38), suggesting that the paracrine effects of estrogen in the brain microenvironment are likely to involve other cell populations and mechanisms. Here we investigated the role of reactive astrocytes as they are known to surround and infiltrate BM in human and experimental models (39-42), and astrocytes play important roles in mediating the responses to estrogen in the normal and injured brain (16, 21, 43-45).We distinctly detected ERα in stromal cells surrounding human breast cancers, and double immunofluorescence staining demonstrated that this ER+ stroma is comprised of GFAP+ reactive astrocytes. This stromal expression of ERα is not routinely evaluated during diagnosis of human breast tumors or their metastases; however, it could be relevant if a correlation between stromal ERα expression, prognosis, and/or treatment response could be addressed in women with brain metastatic breast cancer.

Our results demonstrate that E2-treated human and mouse astrocytes promote proliferation, migration and invasion of 231BR-EGFP cells *in vitro*, in part through the upregulation of EGFR ligands. We demonstrate that this effect is abolished by 4-OH-TAM and ICI, indicating that the paracrine action of E2 depends on astrocytic ERs but the contribution of ERα and ERβ to each phenotype remains unknown. Previous studies have extensively deciphered signaling downstream of EGFR activation in 231BR-EGFP cells and shown that EGFR activation is critical for migration and invasion *in vitro*, and for brain metastatic colonization *in vivo* (31). Since EGFR overexpression is a known risk factor for BM (7) particularly in TN tumors, it is likely that increased levels of EGFR ligands by astrocytes in pre-menopausal women could play a critical role in the ability of TN EGFR expressing brain metastases to colonize the brain.

The paracrine actions of estrogen observed in 231BR-EGFP cells are likely to involve molecules downstream of EGFR activation as well as other unidentified pathways. We show that co-culture with E2-treated astrocytes leads to global changes in gene expression in 231BR-EGFP cells, including S100A4, and that S100A4 is required to mediate the paracrine effects of estrogen *in vitro* and *in vivo*. S100A4 is highly expressed in metastatic tumor cell lines (46) and it exhibits its prometastatic role via affecting apoptosis, cytoskeletal integrity, matrix metalloproteinases (MMPs), tumor-related transcription factors, and stromal factors (33, 46,47). Interestingly, the 231BR-EGFP cells do not express S100A4 endogenously, but only upregulate its expression in response to co-culture with E2-treated astrocytes, further demonstrating that the paracrine action of estrogen can facilitate metastasis. Given the complex bi-directional signaling between astrocytes and breast cancer cells (48-50), further analyses are required to determine the extent to which other genes (both in astrocyte and breast cancer cells) participate in this process.

In conclusion, we have demonstrated that estrogen depletion significantly reduces brain metastatic burden in a TN experimental model *in vivo* and have provided a novel mechanism whereby estrogen acting on ER+ astrocytes, promotes migration, invasion and proliferation of otherwise estrogen-unresponsive TN brain metastatic cells (Figure 7). Importantly, our study suggest that ovarian estrogen depletion and aromatase inhibitors could be of value for the prevention of BM in women with TN EGFR+ tumors at high risk of BM.

METHODS

Human-derived BM

De-identified human samples were obtained from archival paraffin embedded tissue from consenting donors, under approved IRB protocols at the University of Colorado COMIRB.

Cell lines and shRNAs

A brain metastatic derivative of the TN breast cancer cell line MDA-MB-231 transduced with EGFP (231-BR-EGFP) authenticated and free of mycoplasma was maintained as described (51). Human fetal brain neural stem cell line K048 (28) was generously provided by Dr. Ping Wu and maintained as described (52). shRNAs targeting S100A4 (TRCN0000053608, TRCN0000053609 and TRCN0000053608) and a nontargeting control (SHC0002) in the pLKO.1 vector was purchased from a Sigma Mission shRNA library.

Primary astrocyte cultures

Murine cortical primary astrocytes were cultured from postnatal day 1-3 pups as described (51,52). Astrocyte-enriched glial cell cultures were checked for purity and only preparations with >90% GFAP+ cells were used. To obtain 10X concentrated astrocytic-conditioned media (CM), 100% confluent astrocyte cultures were rinsed and incubated for 72 h with serum-free media containing different hormonal treatments. Supernatants were collected and cleared from cell debris and then concentrated by passing it through a 3000 Dalton cutoff centrifuge tube (Millipore) until volume was 1/10 of the initial volume. CM was used immediately or stored at –80C.

Co-culture proliferation assays

Astrocytes were treated with either vehicle (ethanol, OH), 10 nM E2 alone, or in combination with anti-estrogens ICI (100 nM) or 4-OH-TAM, 1 μM) in 0.1% BSA containing serum-free phenol free DMEM. After 24h, 4000 231BR-EGFP cells diluted in 100 μl serum-free media were added on top of astrocytes and allowed to attach for 6h. Four fields per well and 4 wells per treatment were imaged every 4h for up to 6 days using an IncuCyte™ ZOOM Live Cell Imaging System (Essen BioScience) and the percentage of green confluence was calculated over time. Proliferation assays in the absence of an astrocyte-feeding layer were performed in 5% charcoal-stripped FBS (5% CSFBS) containing DMEM.

Co-culture experiments for analysis of brain metastatic cell gene expression and q-RT-PCR

Astrocytes were grown until 100% confluent, then treated with vehicle or 10 nM E2 containing 0.1% BSA serum-free phenol free DMEM for 24 h. 1×10^6 231BR cells were plated on top of OH− (n=3) or E2− (n=3) treated astrocytes or in 1% CS-FBS phenol free DMEM containing OH (n=3) or 10 nM E2 (n=3) in the absence of astrocytes, and incubated for additional 24 h. All samples were sorted in a MoFlo XDP100 (Beckman Coulter) and sorted cells were collected directly in RNA lyses buffer for RNA isolation (RNAqueous-MicroKit). CDNA for qRT-PCR was synthesized using the MuLV reverse transcriptase (Applied Biosystems). β-actin or GAPDG were used for normalization. The relative mRNA levels were calculated using the comparative Ct method (Ct).

Gene Expression profiling

Integrity of triplicate RNA samples was confirmed on a Bioanalyzer (Agilent). The cDNA was generated according to the GeneChip Expression Analysis Technical Manual (Affymetrix). Labeled complementary RNA was made using the GeneChip_IVT Labeling Kit (Affymetrix), fragmented, and hybridized to Human Gene 1.1 ST Arrays. Probe intensities were exported into Partek Genomics Suite (v6.6, Partek, Inc. St. Louis, MO) where RMA normalization was applied, resulting in $\log_2$-transformed expression intensities for each transcript in each sample. Data were filtered using a 1.5-fold change cutoff and a *P* value of 0.05. Microarray data access # GSE71272.

Migration Assays

231BR-EGFP cells were serum starved for 6 h and 40.000 cells per well were plated on a 96-well Essen ImageLock plate. Adhered cells were starved in serum-free media for 16 h and a scratch wound performed using a 96-pin WoundMaker and then treated with hormones or astrocytic CM. Wound images were taken every 4h for 24h and the wound width calculated at each time point. In experiments using lapatinib, cells were pretreated with 1 μM lapatinib or DMSO controls for 6 h prior to scratch wound. Each treatment was performed in 4-biological replicates in at least two independent experiments.

Invasion assays

Cells were plated in matrigel-coated plates, a scratch wound made and filled with 4 μg/ml Matrigel and treated as in migration assays. Relative wound density was calculated for each time point. Alternatively, invasion was measured in Boyden chamber assays: 231BR-EGFP cells were serum-starved for 6h and then 200,000 cells were plated on top of growth factor-reduced Matrigel-coated boyden chambers (BD-Pharmingen). CM from hormonally treated-astrocytes was used as chemoattractant. Cells were allowed to invade for 24 h, the invading cells fixed on the opposite side of the filter and stained using crystal violet. Percentage of the filter covered by invading cells was calculated using Image J. Each treatment was performed in triplicate in at least two independent experiments.

Reagents

Primary antibodies included rat anti-GFAP (Invitrogen, CA); α-tubulin (Sigma-Aldrich, St. Louis, MO, USA), Estrogen Receptor α (C1355) (Millipore, Temecula, CA), Estrogen Receptor β, clone 68-4 (Millipore), S100A4 (Abcam), Pan-cytokeratin MNF116 (Dakocytomation, Denmark); Phospho-EGF Receptor (Tyr1068) and total EGFR (Cell Signaling, Boston, MA). For western blot, secondary antibodies were Alexa-fluor 680 Anti-Rabbit or Anti-Mouse IgG (Invitrogen, NY) detected using an Odyssey Infrared Imaging System (Licor Biosciences, Lincoln, NE). For immunohistochemistry, secondary antibodies were anti-mouse Alexafluor-488 or anti-rabbit Alexafluo-555 (Invitrogen). ER antagonists included 4-OH-tamoxifen (Sigma-Aldrich) and ICI 182780 (Tocris bioscience; R&D systems, Minneapolis, MN). The EGFR/HER2 inhibitor Lapatinib was purchased from Selleckchem (Houston, TX).

Experimental BM

Animal studies were approved by the University of Colorado Institutional Animal Care and Use Committee. BM were developed by injecting 175,000 231BR-EGFP cells in 100 μl PBS in the left ventricle of ovariectomized 5-7 week old female nu/nu mice (Charles River). Randomly assigned mice were implanted with pellets containing either E2 (1mg) or placebo, two days before tumor inoculation. The dose of E2 used in these studies is required to promote tumor growth of estrogen-dependent breast cancer cells in nude mice (53) and it is within serum-levels in pre-menopausal women (~50-150pg/ml)(54) . Letrozole is an aromatase inhibitor known to cross the BBB; here it was used to prevent the local production of E2 in the brain. Letrozole (Selleck chemical, Houston TX) was diluted in 0.3% hydroxyl-propyl cellulose at 0.2 mg/ml and 50 μl were injected subcutaneously daily (10μg/day). Metastatic brain burden was measured using high-resolution T2-weigthed and gadolinium enhanced T2-weigted-MRI at 25 days post-injection. Mice were euthanized 28 days after tumor cell injection, and the brains were removed at necropsy. For quantification of micro-metastases, six hematoxylin and eosin (H&E)–stained serial sections (10-μm-thick), one every 300 μm in a sagittal plane through the right hemisphere of the brain were analyzed using an ocular grid (4X objective). Every micrometastases (300 μm) along the longest axis, respectively) in each section was tabulated by an investigator blinded to the experimental groups.

MRI

Animals were injected with 0.4 mmol/kg gadolinium contrast Multihance (gadobenate dimeglumine, Bracco Diagnostic) via tail vein. Animals were inserted into a Bruker 4.7 Tesla MRI PharmaScan (Bruker Medical) under 2-2.5% isoflurane. High-resolution RARE (rapid acquisition with relaxation enhancement) T2-weighted images with fat suppression were obtained (TR/TE= 4000/ 80 ms) followed by a MSME (multi slice multi echo) T1-weighted sequence (TR/TE= 700/ 11 ms). All images were obtained in the axial plane, with the field of view of 3 cm, slice thickness 1 mm, number of slices 16, matrix size 256×256. In-plane resolution was 90 μm. All images were acquired and analyzed (for lesion numbers and diameters) using Bruker ParaVision (v4.0) software (55), by an investigator blinded to the experimental groups.

Statistical Analysis

Statistics were done using Graphpad Prism 6.0 software. One way ANOVA or repeated measured ANOVA followed by multiple comparison post hoc tests were used when samples met variance and normality tests. P values <0.05 were considered significant. Chi-square was used to compare frequency of MRI-detectable metastases. Number of MRI detectable metastases and median numner of micrometastases were analyzed using one-way non-parametric t-test (Mann-Whitney) or ANOVA (Kruskal Wallis) tests followed by Dunn's multiple comparison test. For animal experiments, sample size was calculated at 80% power, two sided tests and α=0.05.

Supplementary Material

Refer to Web version on PubMed Central for supplementary material.

ACKNOWLEDGMENTS

REFERENCES

1. Cheng X, Hung MC. Breast cancer brain metastases. Cancer metastasis reviews. 2007; 26(3-4):635–43. [PubMed: 17717635]

2. Brufsky AM, Mayer M, Rugo HS, Kaufman PA, Tan-Chiu E, Tripathy D, et al. Central nervous system metastases in patients with HER2-positive metastatic breast cancer: incidence, treatment, and survival in patients from registHER. Clinical cancer research : an official journal of the American Association for Cancer Research. 2011; 17(14):4834–43. [PubMed: 21768129]

3. Kodack DP, Askoxylakis V, Ferraro GB, Fukumura D, Jain RK. Emerging strategies for treating brain metastases from breast cancer. Cancer Cell. 2015; 27(2):163–75. [PubMed: 25670078]

4. Boogerd W, Vos VW, Hart AA, Baris G. Brain metastases in breast cancer; natural history, prognostic factors and outcome. J Neurooncol. 1993; 15(2):165–74. [PubMed: 8509821]

5. Braccini AL, Azria D, Thezenas S, Romieu G, Ferrero JM, Jacot W. Prognostic factors of brain metastases from breast cancer: Impact of targeted therapies. The Breast. 2013; 22(5):993–8. [PubMed: 23831232]

6. Evans AJ, James JJ, Cornford EJ, Chan SY, Burrell HC, Pinder SE, et al. Brain metastases from breast cancer: identification of a high-risk group. Clin Oncol (R Coll Radiol). 2004; 16(5):345–9. [PubMed: 15341438]

7. Hicks DG, Short SM, Prescott NL, Tarr SM, Coleman KA, Yoder BJ, et al. Breast Cancers With Brain Metastases are More Likely to be Estrogen Receptor Negative, Express the Basal Cytokeratin CK5/6, and Overexpress HER2 or EGFR. The American Journal of Surgical Pathology. 2006:1097–104. [PubMed: 16931954]

8. Kaal ECA, Niël CGJH, Vecht CJ. Therapeutic management of brain metastasis. The Lancet Neurology. 2005; 4(5):289–98. [PubMed: 15847842]

9. Lin NU, Bellon JR, Winer EP. CNS Metastases in Breast Cancer. JCO. 2004; 22(17):3608–17.

10. Tham Y-L, Sexton K, Kramer R, Hilsenbeck S, Elledge R. Primary breast cancer phenotypes associated with propensity for central nervous system metastases. Cancer. 2006; 107(4):696–704. [PubMed: 16826579]

11. Lin NU, Vanderplas A, Hughes ME, Theriault RL, Edge SB, Wong Y-N, et al. Clinicopathologic features, patterns of recurrence, and survival among women with triple-negative breast cancer in the National Comprehensive Cancer Network. Cancer. 2012 n/a-n/a.

12. Lee YT. Breast carcinoma: pattern of metastasis at autopsy. J Surg Oncol. 1983; 23(3):175–80. [PubMed: 6345937]

13. Lee SS, Ahn J-H, Kim MK, Sym SJ, Gong G, Ahn SD, et al. Brain metastases in breast cancer: prognostic factors and management. Breast Cancer Res Treat. 2007; 111(3):523–30. [PubMed: 17990100]

14. Tsukada Y, Fouad A, Pickren JW, Lane WW. Central nervous system metastasis from breast carcinoma. Autopsy study. Cancer. 1983; 52(12):2349–54. [PubMed: 6640506]

15. Hung MH, Liu CY, Shiau CY, Hsu CY, Tsai YF, Wang YL, et al. Effect of age and biological subtype on the risk and timing of brain metastasis in breast cancer patients. PLoS ONE. 2014; 9(2):e89389. [PubMed: 24586742]

16. García-Ovejero D, Veiga S, García-Segura LM, Doncarlos LL. Glial expression of estrogen and androgen receptors after rat brain injury. The Journal of Comparative Neurology. 2002; 450(3):256–71. [PubMed: 12209854]

17. Morissette M, Le Saux M, D'Astous M, Jourdain S, Al Sweidi S, Morin N, et al. Contribution of estrogen receptors alpha and beta to the effects of estradiol in the brain. J Steroid Biochem Mol Biol. 2008; 108(3-5):327–38. [PubMed: 17936613]

18. Pettersson K, Gustafsson J-Å. Role of Estrogen Receptor Beta in Estrogen Action. Annual Review of Physiology. 2001; 63(1):165–92.

19. Razmara A, Sunday L, Stirone C, Wang XB, Krause DN, Duckles SP, et al. Mitochondrial Effects of Estrogen Are Mediated by Estrogen Receptor α in Brain Endothelial Cells. J Pharmacol Exp Ther. 2008; 325(3):782–90. [PubMed: 18354059]

20. Arnold S. Estrogen suppresses the impact of glucose deprivation on astrocytic calcium levels and signaling independently of the nuclear estrogen receptor. Neurobiology of Disease. 2005; 20(1):82–92. [PubMed: 16137569]

21. Barouk S, Hintz T, Li P, Duffy AM, MacLusky NJ, Scharfman HE. 17β-estradiol increases astrocytic vascular endothelial growth factor (VEGF) in adult female rat hippocampus. Endocrinology. 2011; 152(5):1745–51. [PubMed: 21343256]

22. Garcia-Segura LM, Azcoitia I, DonCarlos LL. Neuroprotection by estradiol. Progress in Neurobiology. 2001; 63(1):29–60. [PubMed: 11040417]

23. Garcia-Segura LM, Wozniak A, Azcoitia I, Rodriguez JR, Hutchison RE, Hutchison JB. Aromatase expression by astrocytes after brain injury: implications for local estrogen formation in brain repair. Neuroscience. 1999; 89(2):567–78. [PubMed: 10077336]

24. Montelli S, Peruffo A, Zambenedetti P, Rossipal E, Giacomello M, Zatta P, et al. Expression of aromatase P450AROM in the human fetal and early postnatal cerebral cortex. Brain Res. (0).

25. Yague JG, Muñoz A, de Monasterio-Schrader P, Defelipe J, Garcia-Segura LM, Azcoitia I. Aromatase expression in the human temporal cortex. Neuroscience. 2006; 138(2):389–401. [PubMed: 16426763]

26. Palmieri D, Bronder JL, Herring JM, Yoneda T, Weil RJ, Stark AM, et al. Her-2 overexpression increases the metastatic outgrowth of breast cancer cells in the brain. Cancer research. 2007; 67(9): 4190–8. [PubMed: 17483330]

27. Yoneda T, Williams P, Hiraga T, Niewolna M, Nishimura R. A bone seeking clone exhibits different biological properties from the MDA-MB-231 parental human breast cancer cells and a brain-seeking cloe in vivo and in vitro. J Bone and Mineral Res. 2001; 16:1486–95.

28. Svendsen CN, ter Borg MG, Armstrong RJ, Rosser AE, Chandran S, Ostenfeld T, et al. A new method for the rapid and long term growth of human neural precursor cells. Journal of neuroscience methods. 1998; 85(2):141–52. [PubMed: 9874150]

29. Ma YJ, Berg-Von Der Emde K, Moholt-Siebert M, Hill DF, Ojeda SR. Region-Specific Regulation of Transforming Growth Factor Alpha (TGF Alpha) Gene Expression in Astrocytes of the Neuroendocrine Brain. J Neurosci. 1994; 14:5644–5651. [PubMed: 8083760]

30. Lee E, Sidoryk-Wegrzynowicz M, Yin Z, Webb A, Son D-S, Aschner M. Transforming growth factor-α mediates estrogen-induced upregulation of glutamate transporter GLT-1 in rat primary astrocytes. Glia. 2012; 60:1024–1036. [PubMed: 22488924]

31. Gril B, Palmieri D, Bronder JL, Herring JM, Vega-Valle E, Feigenbaum L, et al. Effect of Lapatinib on the Outgrowth of Metastatic Breast Cancer Cells to the Brain. JNCI J Natl Cancer Inst. 2008; 100(15):1092–103. [PubMed: 18664652]

32. Jenkinson SR, Barraclough R, West CR, Rudland PS. S100A4 regulates cell motility and invasion in an in vitro model for breast cancer metastasis. Br J Cancer. 2004; 90(1):253–62. [PubMed: 14710237]

33. Saleem M, Kweon MH, Johnson JJ, Adhami VM, Elcheva I, Khan N, et al. S100A4 accelerates tumorigenesis and invasion of human prostate cancer through the transcriptional regulation of matrix metalloproteinase 9. Proceedings of the National Academy of Sciences of the United States of America. 2006; 103(40):14825–30. [PubMed: 16990429]

34. Arnold S, Victor MB, Beyer C. Estrogen and the regulation of mitochondrial structure and function in the brain. J Steroid Biochem Mol Biol. (0).

35. Péqueux C, Raymond-Letron I, Blacher S, Boudou F, Adlanmerini M, Fouque MJ, et al. Stromal estrogen receptor-α promotes tumor growth by normalizing an increased angiogenesis. Cancer research. 2012; 72(12):3010–9. [PubMed: 22523036]

36. Iyer V, Klebba I, McCready J, Arendt LM, Betancur-Boissel M, Wu MF, et al. Estrogen promotes ER-negative tumor growth and angiogenesis through mobilization of bone marrow-derived monocytes. Cancer research. 2012; 72(11):2705–13. [PubMed: 22467173]

37. Valastyan S, Weinberg RA. Tumor metastasis: molecular insights and evolving paradigms. Cell. 2011; 147(2):275–92. [PubMed: 22000009]

38. Valiente M, Obenauf AC, Jin X, Chen Q, Zhang XH, Lee DJ, et al. Serpins promote cancer cell survival and vascular co-option in brain metastasis. Cell. 2014; 156(5):1002–16. [PubMed: 24581498]

39. Abbott NJ, Ronnback L, Hansson E. Astrocyte-endothelial interactions at the blood-brain barrier. Nature reviews Neuroscience. 2006; 7(1):41–53. [PubMed: 16371949]

40. Fidler IJ. The role of the organ microenvironment in brain metastasis. Seminars in Cancer Biology. 2011; 21(2):107–12. [PubMed: 21167939]

41. Gril B, Palmieri D, Qian Y, Anwar T, Liewehr DJ, Steinberg SM, et al. Pazopanib inhibits the activation of PDGFRbeta-expressing astrocytes in the brain metastatic microenvironment of breast cancer cells. Am J Pathol. 2013; 182(6):2368–79. [PubMed: 23583652]

42. Kim S-J, Kim J-S, Park ES, Lee J-S, Lin Q, Langley RR, et al. Astrocytes upregulate survival genes in tumor cells and induce protection from chemotherapy. Neoplasia. 2011; 13(3):286–98. [PubMed: 21390191]

43. Azcoitia I, Santos-Galindo M, Arevalo MA, Garcia-Segura LM. Role of astroglia in the neuroplastic and neuroprotective actions of estradiol. Eur J Neurosci. 2010; 32(12):1995–2002. [PubMed: 21143654]

44. Dhandapani KM, Wade FM, Mahesh VB, Brann DW. Astrocyte-Derived Transforming Growth Factor-β Mediates the Neuroprotective Effects of 17β-Estradiol: Involvement of Nonclassical Genomic Signaling Pathways. Endocrinology. 2005; 146(6):2749–59. [PubMed: 15746252]

45. Garcia-Segura LM, Torres-Aleman I, Naftolin F. Astrocytic shape and glial fibrillary acidic protein immunoreactivity are modified by estradiol in primary rat hypothalamic cultures. Brain Res Dev Brain Res. 1989; 47(2):298–302. [PubMed: 2743562]

46. Dahlmann M, Sack U, Herrmann P, Lemm M, Fichtner I, Schlag PM, et al. Systemic shRNA mediated knock down of S100A4 in colorectal cancer xenografted mice reduces metastasis formation. Oncotarget. 2012; 3(8):783–97. [PubMed: 22878175]

47. Wang L, Wang X, Liang Y, Diao X, Chen Q. S100A4 promotes invasion and angiogenesis in breast cancer MDA-MB-231 cells by upregulating matrix metalloproteinase-13. Acta Biochim Pol. 2012; 59(4):593–8. [PubMed: 23162804]

48. Neman J, Choy C, Kowolik CM, Anderson A, Duenas VJ, Waliany S, et al. Co-evolution of breast-to-brain metastasis and neural progenitor cells. Clin Exp Metastasis. 2013; 30(6):753–68. [PubMed: 23456474]

49. Wang L, Cossette SM, Rarick KR, Gershan J, Dwinell MB, Harder DR, et al. Astrocytes directly influence tumor cell invasion and metastasis in vivo. PLoS ONE. 2013; 8(12):e80933. [PubMed: 24324647]

50. Fong MY, Zhou W, Liu L, Alontaga AY, Chandra M, Ashby J, et al. Breast-cancer-secreted miR-122 reprograms glucose metabolism in premetastatic niche to promote metastasis. Nature cell biology. 2015; 17(2):183–94. [PubMed: 25621950]

51. Yoneda T, Williams PJ, Hiraga T, Niewolna M, Nishimura R. A Bone-Seeking Clone Exhibits Different Biological Properties from the MDA-MB-231 Parental Human Breast Cancer Cells and a Brain-Seeking Clone In Vivo and In Vitro. Journal of Bone and Mineral Research. 2001; 16(8): 1486–95. [PubMed: 11499871]

52. Wu P, Tarasenko YI, Gu Y, Huang LY, Coggeshall RE, Yu Y. Region-specific generation of cholinergic neurons from fetal human neural stem cells grafted in adult rat. Nature neuroscience. 2002; 5(12):1271–8. [PubMed: 12426573]

53. Osborne CK, Hobbs K, Clark GM. Effect of estrogens and antiestrogens on growth of human breast cancer cells in athymic nude mice. Cancer research. 1985; 45(2):584–90. [PubMed: 3967234]

54. Stanczyk FZ, Mathews BW, Sherman ME. Relationships of sex steroid hormone levels in benign and cancerous breast tissue and blood: A critical appraisal of current science. Steroids. 2015; 99(Pt A):91–102. [PubMed: 25554581]

55. Frey L, Lepkin A, Schickedanz A, Huber K, Brown MS, Serkova N. ADC mapping and T1-weighted signal changes on post-injury MRI predict seizure susceptibility after experimental traumatic brain injury. Neurological research. 2014; 36(1):26–37. [PubMed: 24107461]
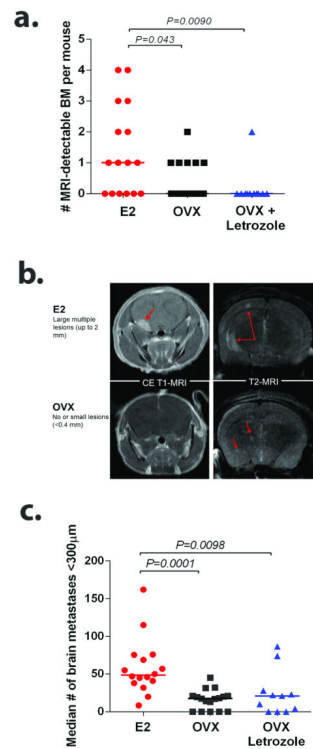
Figure 1. Estrogen depletion decreases experimental breast cancer BM formation

OVX nude mice supplemented with placebo (OVX, n=17), estrogen (E2,n=16) or letrozole (OVX+Letrozole, n=11) were injected intracardially with 175,000 triple-negative 231BR-EGFP cells. Data represents two separate experiments. **a**. Number of MRI-detectable BM per mice in each group. Line designates group median. **b.** Representative contrast-enhanced (CE) T1-weighted and fat-suppressed T2-weighted MRI showing increased number and size of BM in E2-treated mice compared to OVX mice. **c**. Number of micrometastases per brain section (<300 μm). Each dot represents the median per mouse and the line designates the group median. Data was analyzed using non-parametric One Way ANOVA followed by Dunn's multiple comparisons test. Graph shows adjusted P values.
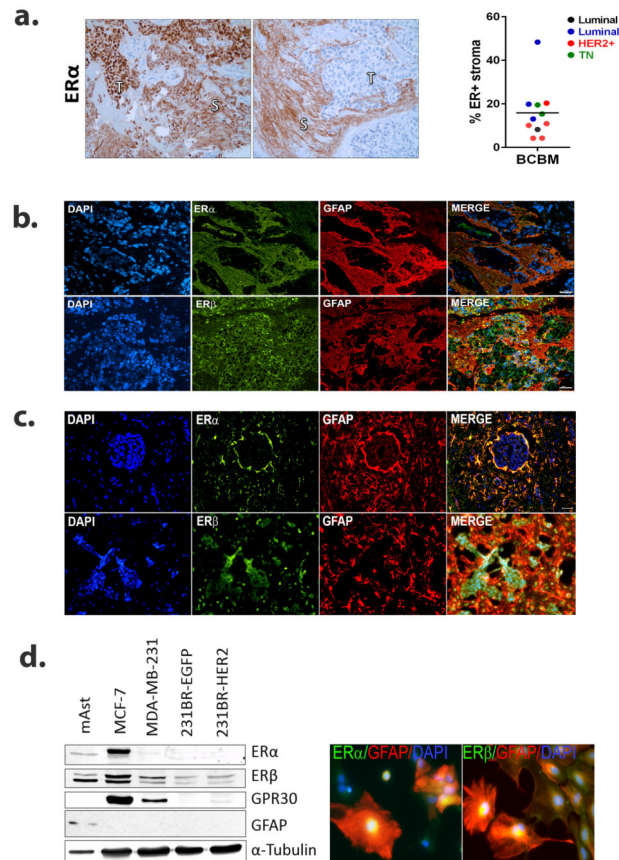
Figure 2. Astrocytes in the brain metastatic microenvironment are ER+

a. ERα is detected in stroma (S) surrounding tumor cells (T) in clinical immunostains from human BM from ER+ and ER− subtypes. Graph shows the percent ERα positive-stained stromal area in immunostained human breast cancer BM (BCBM) (n=12), analyzed using the Aperio system (see Supplementary Figure 1). Colored dots represent different subtypes. **b.** Activated astrocytes (GFAP+) surrounding human BM express ERα and ERβ (green). ERβ is expressed in astrocytes and tumor cells in ER-case. **c.** GFAP+ mouse astrocytes express ERα and ERβ (green) in experimental BM of 231BR-EGFP cells. **d.** *Left:* Western blot shows expression of ERs in mouse primary astrocytes (mAst), ER+ MCF-7 cells, ER− MDA-MB-231 cells and ER− brain metastatic derivatives 231BR-EGFP and 231BR-HER2. α-tubulin is used as loading control. *Right:* Primary mouse astrocytes are reactive *in vitro* (GFAP+, red) and express ERα and ERβ (green). DAPI stains nuclei (blue).
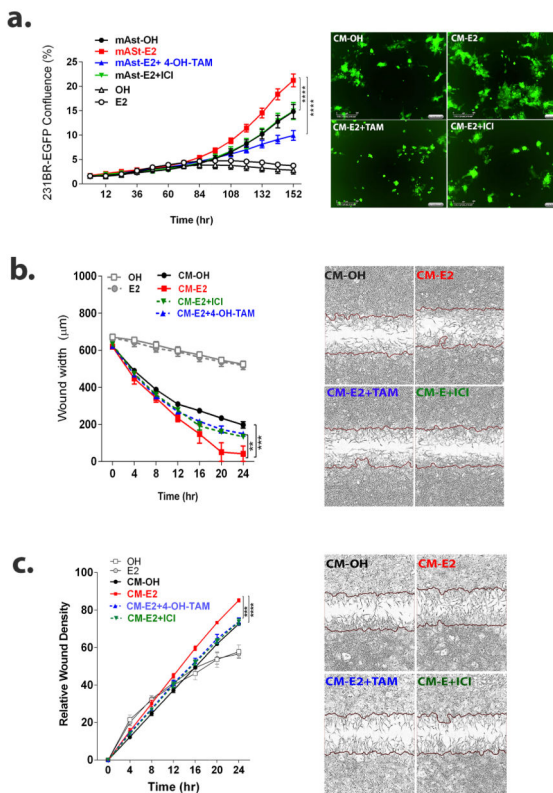
Figure 3. E2-treated astrocytes increase proliferation, migration and invasion of brain metastatic cells in an ER-dependent manner

a. 231BR-EGFP cells were plated on top of a mouse-primary astrocyte monolayer and cultured in serum-free media with vehicle (OH) or E2 alone (10 nM) or E2 in combination with 1 μM 4-OH-Tam (E2+TAM) or 100 nM ICI (E2+ICI). 231BR-EGFP cells were also treated with vehicle (OH) or 10 nM E2 (E2) in 5% CS-FBS media in absence of astrocytes to determine direct effects of E2. Graph shows the average percentage of 231BR-EGFP density ± SEM (n=4 per treatment), representative of at least two independent experiments. P<0.01 CM-OH vs CM-E2 start at 120 h. *Right:* Representative image shows 231BR-EGFP cells at 6 days. **b.** 231BR-EGFP cells were serum-starved overnight and 10X CM of astrocytes treated for 72 h with vehicle (CM-OH) or 10 nM E2 alone (CM-E2) or in combination with 1 μM Tam (CM E2+TAM) or 100 nM ICI (CM E2+ICI), were used as chemoattractant in scratch wound assays. Graph shows wound width (μm) over time. CM-OH vs CM-E2 P<0.01 for each time point after 16 h. *Right:* Representative image of wound at 24 h. **c.** 231BR-EGFP cells were treated as in b, in a modified scratch wound assays (see methods). Graphs shows average relative wound confluence (RWC) ± SEM. RWC is proportional to the amount of cells invading through the ECM-filled wound. CM-OH vs CM-E2 P<0.05 start at 16hr. *Right:* Representative image of wound at 24hrs. For all graphs, **P<0.01, ***P<0.001, ****P<0.0001 indicates the significance at the latest time point in repeated measures ANOVA followed by post-hoc multiple comparisons test.

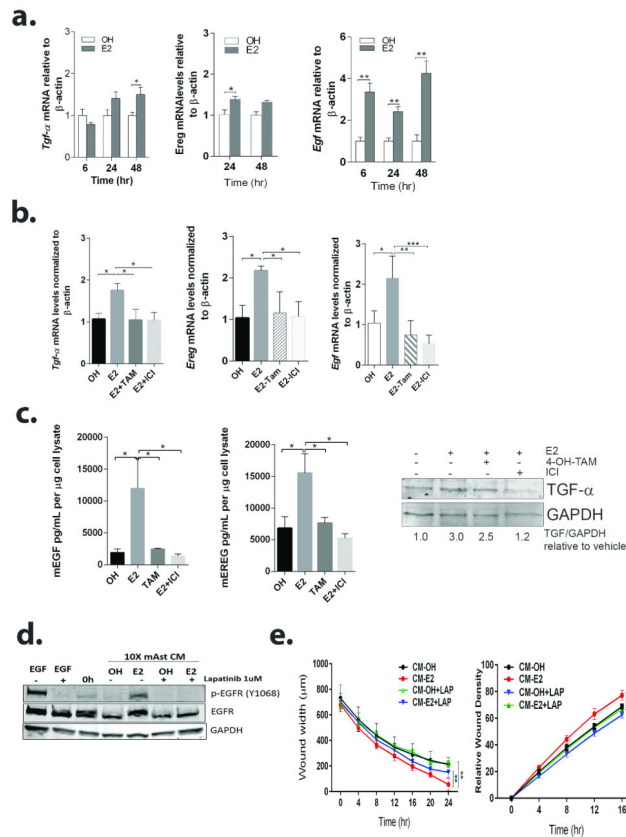**Figure 4. E2 upregulates EGFR ligands in astrocytes and results in EGFR activation in brain metastatic cells**

a. Primary mouse astrocytes were treated with vehicle (OH) or 10 nM E2 for the indicated times and qRT-PCR was used to measure Egf, Tgfα and Ereg mRNA levels. Bars represent fold change mRNA levels normalized to mouse β-Actin mRNA and relative to OH-treated. *P<0.05, **P<0.01 vs. OH-control. n=3. **b.** Astrocytes were cultured in serum-free media containing vehicle (OH) or E2 alone (10 nM) or E2 in combination with 1 μM 4-OH-Tam (E2+TAM) or 100 nM ICI (E2+ICI) for qRT-PCR at 24 h (for Egf and Ereg) or 48 h (for Tgfα). Graph shows mRNA levels normalized to mouse β-actin relative to OH-treated astrocytes. Bars are average ± SEM. **c.** Astrocytes were cultured as in b for 48 h, and cell lysates assessed by ELISA (mEGF, mEREG) or Western blot (TGFα). Graphs shows mEGF and mEREG concentration in 1 μg total cell lysate. Bars are average ± SEM. WB shows precursor TGFα (16KD), GAPDH was used as loading control. Numbers indicate fold change of TGFα/GAPDH relative to OH-treated cells. **d.** 231BR-EGFP cells were starved for 12 h, treated with 1 uM lapatinib or vehicle (DMSO) for 6 h and then stimulated with 10 ng/ml EGF, CM-OH or CM-E2 for 10 min. GAPDH was used as loading control. **e.** 231BR-EGFP cells were plated in uncoated (*left*, migration) or matrigel-coated (*right,* invasion) plates, serum-starved for 16 h and treated with 1 μM lapatinib for 3 h. After scratch wound, invasion well were coated with matrigel and then CM-OH or CM-E2 used as chemoattractant. Graphs show average wound width ±SEM (migration) and average RWD ± SEM (invasion). For all graphs, *P<0.05, **P<0.01, ***P<0.001.
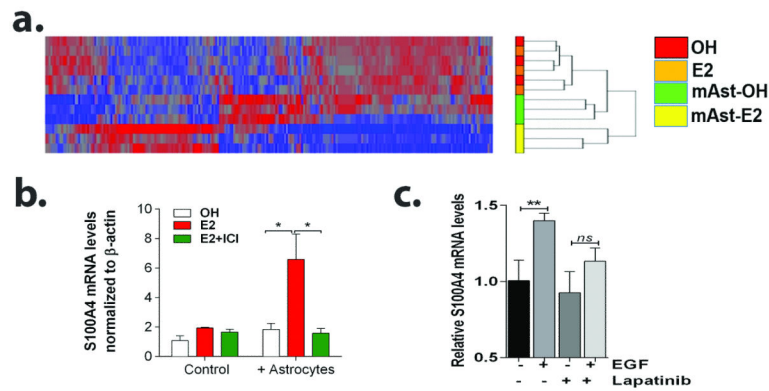
Figure 5. Paracrine action of estrogen through astrocytes results in upregulation of metastasis mediator S100A4 in 231BR-EGFP cells

a. Hierarchical clustering of genes significantly affected by E2-treated astrocytes in sorted 231BR-EGFP cells treated with OH, 10 nM E2 alone, or in co-culture with OH-treated (mASt-OH) or 10 nM E2-treated (mAst) mouse astrocytes. n=3 per group, P<0.05, 1.5 fold change cutoff. **b.** 231BR-EGFP cells were treated with OH, 10 nM E2 alone or in combination with 100 nM ICI , either alone or in co-culture with astrocytes for 24 h. Sorted GFP+ cells were used for qRT-PCR analyses. Graph shows average S100A4 mRNA levels normalized to β-actin and relative to OH-treated cells ± SEM (n=3). Data representative of two independent experiments. **c.** 231BR-EGFP cells were starved for 16 h, pre-treated with 1 uM lapatinib or vehicle for 6 h and then treated with vehicle or 10 ng/ml EGF in 5% charcoal stripped-FBS containing media for 24 h. Graphs shows average S100A4 mRNA levels normalized to GAPDH and relative to vehicle-treated cells ± SEM, **P<0.01.
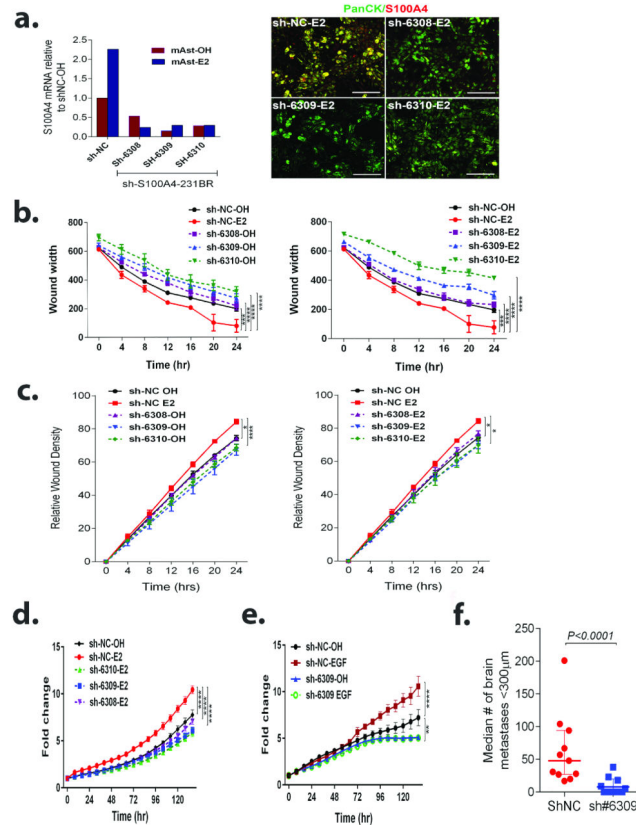
Figure 6. S100A4 knockdown blocks proliferation, migration and invasion of 231BR-EGFP cells in response to E2-treated astrocytes and inhibits brain colonization *in vivo*
a. *Left:* 231BR-EGFP cells expressing scramble control (sh-NC) or S100A4 targeting shRNAS (sh6308, sh6309, sh6310) were co-cultured with OH or E2-treated astrocytes for 24 h and then sorted. Graph shows S100A4 mRNA expression normalized to β-actin and relative to shNC-OH-treated control. Right: Cells were co-cultured as in a, and S100A4 expression assessed by IF. Panel shows merged images of S100A4 (red) and pan-cytokeratin labeling 231BR-EGFP cells (green). Individual channels are shown in Supplementary figure 3. **b.** shNC or shS100A4 cells were serum-starved overnight and CM-OH or CM-E2 was used as chemoattractant in scratch wound assays. Graph shows average wound width ± SEM. **c.** shNC or shS100A4 cells were treated as in b, in a modified scratch wound assay. Graphs shows relative average wound confluence (RWC) ± SEM. **d.** shNC or shS100A4 cells were plated on top of an astrocyte monolayer and cultured in serum-free media with OH, E2, or E2+ICI, and GFP+ confluence measured over time using live imaging. Data represents fold change in GFP+cells confluence relative to day 0± SEM. **e.** shNC or shS100A4 cells were plated in 5% CSFBS containing media and treated with vehicle or 10 ng/mL EGF for 6 days. Graph shows fold change in GFP+ cells relative to time 0 ± SEM (n=4). For all graphs, **P<0.01, ***P<0.001, ****P<0.0001 indicates the significance at the latest time point in repeated measures ANOVA followed by post-hoc multiple comparisons test. **f.** Female OVX nude mice supplemented with estrogen pellets, were injected intracardially with 175,000 sh-NC (n=11) or shS100A4-6309 (Sh#6309) cells and mice euthanized 28 days after injection. Micrometastases (<300 μm) per

brain section in 6 sections through the right hemisphere were quantified. Each dot represents the median per mouse and the line designates the group median. Data was analyzed using Mann-Whitney non-parametric t-test.
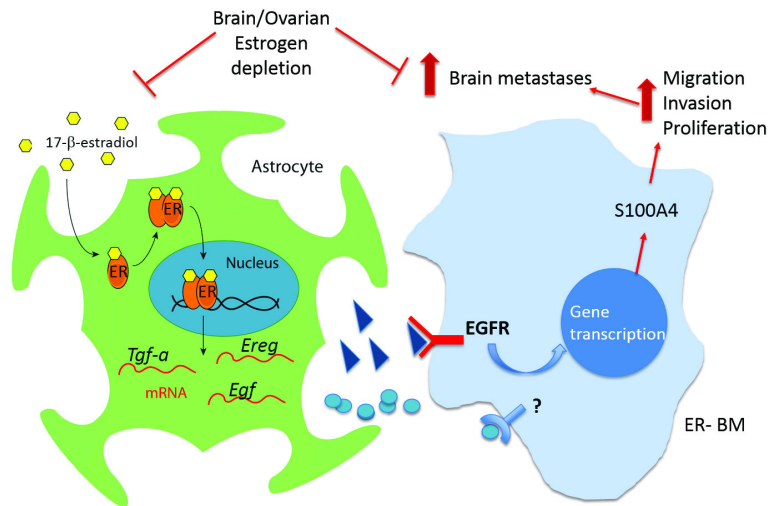
Figure 7. A simplified scheme of the paracrine effects of estrogen in brain metastases
Consistent with the notion that breast cancer cells benefit from normal homeostasis mechanisms at the metastatic site (48, 50), our data supports a novel mechanism whereby brain metastatic cells exploit estrogen signaling though ER+ astrocytes. Estrogen can activate ERs on astrocytes, leading to transcriptional upregulation of EGFR ligands, activation of EGFR on TN EGFR+ brain metastatic breast cancer cells, and upregulation of several metastatic mediators, including S100A4. Given the complex bi-directional interactions between astrocytes and breast cancer cells, it is possible that other factors regulated by ERs in astrocytes and receptors on brain metastatic cells participate in this process. Ovarian and local estrogen depletion decrease brain metastatic colonization of TN EGFR+ 231BR cells *in vivo*, emphasizing the need to consider the brain microenvironment in designing novel therapies for brain metastases and the possibility to extend the use of aromatase inhibitors in the prevention of brain metastases in TN EGFR+ patients.